Numerical Study of a Vertical Axis Wind Turbine with an Inner Cylindrical Deflector

Najm Addin Al-Khawlani[1], Ahmad Fazlizan[1,*], Asmail A. M. Abdalkarem[2], Adnan Ibrahim[1] and Zambri Harun[3]

[1] Solar Energy Research Institute, Universiti Kebangsaan Malaysia, Bangi, 43600, Malaysia

[2] Mechanical Department, Faculty of Engineering, Azzaytuna University, Tarhuna, P.O. Box 5338, Libya

[3] Department of Mechanical and Manufacturing Engineering, Universiti Kebangsaan Malaysia, Bangi, 43600, Malaysia

INFORMATION

Keywords:
Vertical-axis wind turbine (VAWT)
cylindrical deflector
aerodynamics performance
computational fluid dynamics (CFD)
torque optimization

DOI: 10.23967/j.rimni.2025.10.63679

Revista Internacional de Métodos Numéricos para Cálculo y Diseño en Ingeniería

Numerical Study of a Vertical Axis Wind Turbine with an Inner Cylindrical Deflector

Najm Addin Al-Khawlani[1], **Ahmad Fazlizan**[1,*], **Asmail A. M. Abdalkarem**[2], **Adnan Ibrahim**[1] **and Zambri Harun**[3]

[1]Solar Energy Research Institute, Universiti Kebangsaan Malaysia, Bangi, 43600, Malaysia

[2]Mechanical Department, Faculty of Engineering, Azzaytuna University, Tarhuna, P.O. Box 5338, Libya

[3]Department of Mechanical and Manufacturing Engineering, Universiti Kebangsaan Malaysia, Bangi, 43600, Malaysia

ABSTRACT

Climate change demands innovative renewable energy solutions, with wind energy emerging as a key resource. Vertical-axis wind turbines (VAWTs) are particularly suited for low-speed, turbulent wind environments due to their ability to capture wind from all directions. However, VAWTs face aerodynamic difficulties, especially at the downwind, where problems like negative torque and decreased efficiency are frequent. This study explores a novel solution for enhancing VAWT performance by incorporating an inner cylindrical deflector aimed at optimizing airflow around the blades. Using computational fluid dynamics (CFD) simulations, the study focuses on a three-bladed H-type VAWT with an airfoil profile of NACA0018 at a turbine diameter of 1 m. The simulations begin by evaluating a bare turbine arrangement, which shows negative torque beginning at an azimuth angle of about 165 degrees onwards. When a cylindrical deflector of different diameters is introduced, the torque coefficient and overall performance are greatly enhanced by a 0.3-meter diameter. The cylindrical deflector's effectiveness is demonstrated by the 15% increase in power coefficient C_p that results from its inclusion. These results highlight how an inner cylindrical deflector could be a useful addition to VAWTs, resolving significant inefficiencies while preserving a positive angle of attack. This strategy offers a way forward for more effective VAWT designs in renewable energy systems in addition to increasing energy output. To enhance the efficiency of vertical-axis wind turbines (VAWTs) for both urban and rural applications, future research could investigate different configurations and empirically confirm these findings.

OPEN ACCESS

Received: 21/01/2025

Accepted: 10/03/2025

Published: 20/04/2025

DOI
10.23967/j.rimni.2025.10.63679

Keywords:
Vertical-axis wind turbine (VAWT)
cylindrical deflector
aerodynamics performance
computational fluid dynamics (CFD)
torque optimization

*Correspondence: Ahmad Fazlizan (a.fazlizan@ukm.edu.my).

Nomenclature

A	Rotor swept area (m^2)
C	Blade chord (m)
C_m	Torque coefficient
C_p	Power coefficient
d	Rotor diameter (m)
P	Power (W)
T	Torque (N·M)
Δt	Time step size (s)
ρ	Air density (kg/m^3)
θ	Azimuth angle (degree)
μ	Dynamic viscosity (Pa·s)
U_∞	Free-stream wind velocity (m/s)
ω	Angular velocity (rad/s)
$y+$	Non-dimensional wall distance

Abbreviations

2D	Two-Dimensional
AoA	Angle of attack
CFD	Computational Fluid Dynamics
HAWT	Horizontal-axis wind turbine
Re	Reynolds number
SST	Shear Stress Transport
SST k-ω	Shear Stress Transport k-omega
TSR	Tip speed ratio (λ)
URANS	Unsteady Reynolds-averaged Navier–Stokes
VAWT	Vertical-axis wind turbine

1 Introduction

Renewable energy is essential in combating the worldwide issue of climate change by offering sustainable substitutes for fossil fuels [1]. Among different renewable energy sources, wind energy has become one of the most practical choices for producing electricity. Wind turbines, devices that transform the wind's kinetic energy into mechanical power, are generally divided into two primary types: horizontal-axis wind turbines (HAWTs) and vertical-axis wind turbines (VAWTs). HAWTs are the most widely utilized type, featuring blades that spin around a horizontal axis and are oriented to face directly into the wind. HAWTs are known for their high efficiency, often exceeding 70% due to their aerodynamic design and ability to capture wind energy effectively at higher elevations [2]. VAWTs are characterized by blades rotating around a vertical axis, a design that enables efficient wind to capture from any direction without requiring positional adjustments. While VAWTs generally operate at lower efficiencies, ranging from 50% to 60%, they offer unique advantages in specific applications [3].

Over the last few years, VAWTs have been the center of attention for research, especially for the urban environment and low wind speed applications. VAWT generally has a simple design, easier construction, and lower costs. The omnidirectional nature of VAWT enables them to harness wind from all directions, which is one of their significant advantages [4,5]. This feature makes them better suited for turbulent and complex wind conditions compared to the more established HAWTs. However, they suffer low efficiency with complex aerodynamic characteristics [6]. The challenge relates to the varying angles of attack (AoA) throughout the turbine's revolution and the resulting fluctuations in aerodynamic forces acting on the blades, especially downwind of the turbine [7]. When a blade moves into the downwind position, the AoA can become negative, leading to a reduction in lift and potentially generating negative torque [8]. This negative torque occurs because the aerodynamic forces acting on the blade are no longer aligned in a manner that contributes positively to rotation; instead, they can act against it.

Numerous efforts have been undertaken to enhance the efficiency of these energy conversion systems. Research has focused on flow augmentation technologies, including diffusers, ducts, deflectors, and guide vanes, to optimize turbine performance [9,10]. It has been demonstrated that adding deflectors to VAWTs greatly improves their performance by increasing their power output and aerodynamic properties. Wong et al. (2019) demonstrated that directing and accelerating airflow by approximately 18% more than the incoming wind, through the use of an omni-directional deflector, led to an increased coefficient of power [11]. Jiang et al. (2020) explored the effects of front deflector placement on local flow conditions in vertical-axis wind turbines using computational fluid dynamics (CFD) simulations [12]. Their study optimized key parameters such as deflector position, angle, and distance from the turbine. The results indicated that proper deflector placement significantly improved local aerodynamic conditions and enhanced turbine performance and efficiency. More recently, Vijay et al. (2023) conducted a comprehensive examination of the design, fabrication, and testing of a VAWT featuring integrated wind deflectors [13]. Their project involved transitioning from a Darrieus-type turbine to a Savonius-type turbine, necessitating a complete redesign of the components to enhance torque and rotational speed. Through CFD analysis, they pinpointed critical factors, such as blade positioning and deflector shape, that significantly improve efficiency. Their research underscores the vital role of design optimization in achieving high-performance VAWTs. Similarly, Iliev et al. (2024) study presented an innovative frontal guiding device composed of deflectors and cylindrical guide vanes [14]. Their findings demonstrated that this guiding mechanism could improve turbine efficiency by a factor of 2.5. By showcasing the effectiveness of deflectors in enhancing performance metrics and comparing the operating curves of their design with those of similar wind turbines, they set the stage for future advancements in turbine design. When we combine these studies with the rest of the literature addressing deflector integration in VAWTs, it can be concluded that deflectors are critical in achieving higher turbine efficiencies among different designs. Table 1 presents a summary of findings from other studies performed for insight into the effects of these deflectors on VAWT performance.

Table 1: Summary of recent study on VAWT with flow augmentation device

Ref.	Aim of the study	Methodology	Main findings	Significance & Potential research areas
[15]	To address noise issues in small VAWTs and assess deflector impact	CFD simulation	Deflectors reduce noise while improving turbine efficiency, helping make VAWTs more acceptable publicly	Shows deflectors can make VAWTs quieter and more efficient.

(Continued)

Table 1 (continued)

Ref.	Aim of the study	Methodology	Main findings	Significance & Potential research areas
[16]	To reduce aerodynamic losses in VAWTs using a combined actuator	CFD simulation with plasma actuators	Deflector at 45° angle increases power by 13.37%; with plasma actuators, power increase reaches 45.68%	Indicates deflectors, especially with plasma actuators, greatly boost efficiency.
[17]	To improve torque in small-scale VAWTs	CFD simulation	Adding a stator deflector increases torque production by 70%, beneficial for small, remote turbines	Shows deflectors can optimize the small turbines' performance.
[18]	To find the optimal angle for a deflector on a micro-VAWT	Experimental study	A 70° deflector angle significantly improves rotor speed, torque, and power	Highlights the importance of deflector angle in small VAWTs.
[19]	To examine different deflector setups on rotor dynamics	CFD simulation	Proper deflector placement improves energy capture and reduces turbulence	Adds evidence for optimized deflector positioning to boost performance.
[20]	To analyze a double-deflector design in an H-Darrieus VAWT for performance optimization	CFD simulation	Double-deflector configuration outperformed single and bare turbines	
[21]	To investigate the impact of flow deflector plates on crossflow wind turbine performance	Experimental study	Three deflector plates increased performance by ∼60% at maximum output and sustained 50% higher output than bare CFWTs under varying wind directions	Highlights the role of deflectors in mitigating drag effects.

Moreover, the integration of guide vanes in VAWTs shows great promise for improving efficiency, especially in space-constrained urban and suburban areas. Kołodziejczyk et al. (2022) conducted a numerical study on VAWTs with guide vanes, demonstrating that specific rotor and guide vane configurations could yield a higher power coefficient than traditional VAWTs, making them feasible for practical applications [22]. Al-Gburi et al. (2023) analyzed the aerodynamic efficiency of Savonius wind turbines, implementing a novel optimization method that incorporated guide gap flow into the blade design [23]. Their results, obtained through 3D ANSYS CFX simulations, showed a 22.8% improvement in power coefficient over conventional designs, underscoring the impact of geometric optimization and guide vanes on turbine performance. In another study, Habibullah et al. (2023) introduced Omni-Directional Guided Vanes (ODGVs) to enhance self-starting capability. and lower the cut-in speed of VAWTs [24]. Their CFD analysis revealed that optimized ODGV configurations could C_p and C_m by up to 58%, highlighting guide vanes as a key innovation for improving VAWT operational characteristics across diverse applications.

Despite the success of exterior deflectors and guide vanes in improving VAWT performance, a persistent challenge remains—the generation of negative torque on the downwind side, which reduces overall efficiency. Most previous studies have focused on external deflector designs to manipulate airflow around the turbine and increase upwind torque [7,25–27]. While these approaches have had some success, they take up a lot of space and are easily affected by changing weather conditions. Additionally, these external solutions primarily affect the upwind side, leaving the complex flow patterns on the downwind side largely unaddressed.

One crucial gap in current research is the lack of investigation into internal flow control strategies for managing airflow patterns within the turbine. This study proposes a novel internal cylindrical deflector, placed around the turbine shaft, to reshape airflow on the downwind side, mitigating the adverse effects of negative torque. By modifying the flow pattern internally, this approach offers a more compact and integrated solution that improves the aerodynamic performance of VAWTs and enhances the consistency of torque generation across all azimuth angles.

2 CFD Methodology

2.1 Model Geometry

To examine the effect of the inner cylinder deflector on aerodynamic efficiency, a 3-bladed H-type VAWT with symmetric NACA0018 airfoils was employed. Each blade has a chord length, C of 0.1 m, and the turbine features a diameter of 1 m. The comprehensive specifications of the VAWT are provided in Table 2. Fig. 1 illustrates the initial state of the 3 blades. The azimuth angle of a blade is represented by θ, with Blade 1's position defined based on its starting location at the beginning of one cycle. In this research, the starting position of Blade 1 is defined as θ = zero° [28].

Table 2: Geometrical parameter of the VAWT

Parameter	Value
Number of blades (-)	3
Blade Airfoil (-)	NACA0018
Blade chord (m)	0.1
Radius (m)	0.5
Rotational Speed, ω (rad/s)	24–56
Wind speed, U_∞ (m/s)	8
Tip speed ratio, λ (-)	1.5–3.5

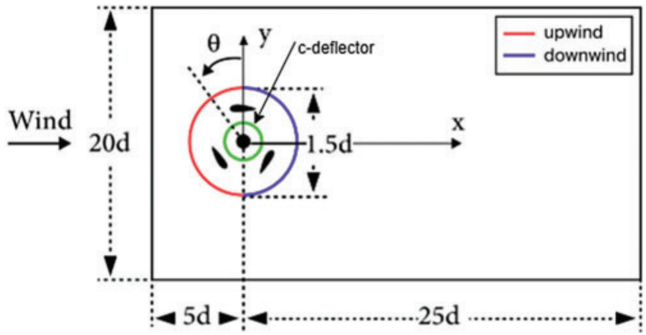

Figure 1: Diagram of various mesh zones in the computational domain of two dimensions (2D)

2.2 Computational Domain and Meshing

The computational domain is composed of a rotating region housing the wind turbine and a stationary outer domain that surrounds the rotating zone. The rotating region has a diameter of 1.5 D, while the stationary rectangular region extends to 30 D in length and 20 D in width [29]. To enable an accurate simulation of the turbine's rotation in the computational domain, a non-conformal interface with a sliding mesh is employed between the two regions [30]. This interface allows for the moving core of the turbine to rotate in a way that is similar to the motion it would have in the real world while keeping the computational domain outside the turbine stationary. In addition, we put inside the rotating domain, a cylindrical deflector which is placed around the shaft and represented by a circle. Rezaeiha et al. (2017) investigated the impact of the blockage ratio on two-dimensional vertical-axis turbine simulations [29]. In Razaeiha's investigation, the blockage ratio, which is the ratio of the turbine diameter to the domain diameter, was chosen at 5%. A 5% blockage ratio leads to negligible artificial fluid acceleration because of asymmetric boundary conditions, according to this systematic analysis, which took into account turbines with solidity and tip speed ratios comparable to those in the current work. When the blockage ratio was lowered from 5% to 1.43%, the study discovered that the computed power coefficient, C_p changed by just 0.2%, suggesting that the turbine's aerodynamic performance was barely affected. Grid generation is a fundamental component of numerical simulations.

Wind turbine simulation can be more accurate with high-quality grids. As a result, a structured grid is selected for the inner revolving zone and the outer stationary domain in all circumstances (see Fig. 2), where the element size for the rotating region is 0.004 m and for the fixed region is 0.1 m. As illustrated in Fig. 2, to distinctly analyze the impact of the presence of a cylindrical deflector on the efficiency of the VAWT, we build another grid without a cylinder deflector for comparison computation. Moreover, the precision of the simulation conducted using the Transition SST turbulence model is tied to the wall distance, defined in dimensionless terms as $y+$, which is a critical parameter for turbulence modeling. The $y+$ value is computed as $y+ = \rho u\tau y/\mu$, where $u\tau$ is the friction velocity, ρ is density, y is the boundary layer length, and μ is dynamic viscosity. The boundary layer grid is utilized not only to accommodate the turbulence model requirements but also to assure the overall accuracy of the simulation. This means that on both the cylindrical deflector surface and the airfoil surface, a boundary layer grid is present, with first-layer grid heights defined as 10^{-4} and 10^{-5}, respectively, so that $y+$ is less than 1.

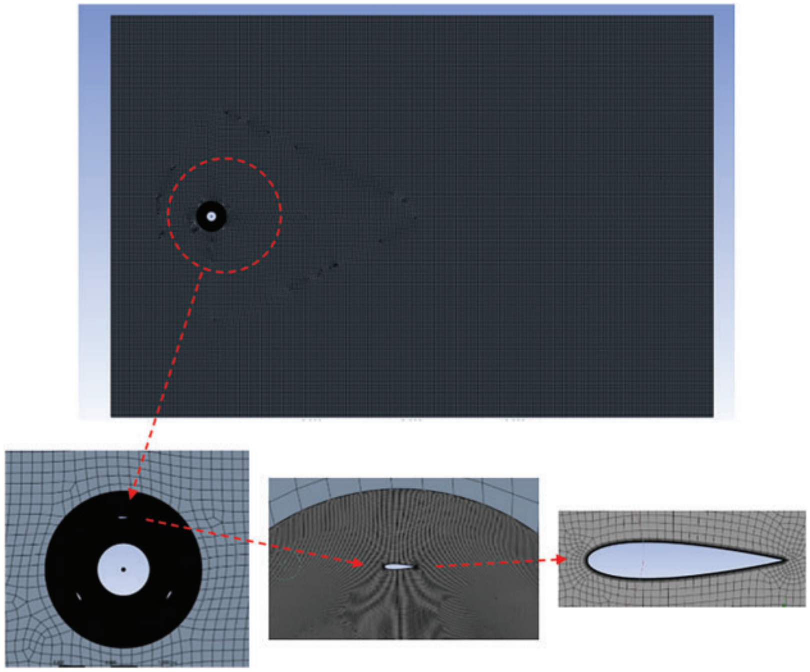

Figure 2: Details of the meshing include the inner region, the mesh close to the airfoil, and the whole mesh in the computational domain

2.3 Mesh Independence Study

A mesh independence study was conducted to ensure the reliability of the simulation results. Five different mesh configurations (M1–M5) were tested by varying the element sizes in the stationary and rotating regions. The power coefficient, C_p at TSR = 3 was used as the primary indicator for evaluating mesh independence. Table 3 and Fig. 3 present the results for each mesh configuration. The difference in C_p between M4 and M3 is less than 0.5%, while there is no difference (0.00%) between M4 and M5, confirming that M4 provides sufficient accuracy at a reasonable computational cost.

Table 3: Mesh independence results for power coefficient, C_p at TSR = 3

Mesh	Stationary region element size (m)	Rotating region element size (m)	Total elements	Power coefficient, C_p	Difference (%)
M1	0.2	0.01	89,122	0.317	–
M2	0.1	0.006	247,124	0.321	1.26%
M3	0.1	0.005	432,564	0.323	0.62%
M4	0.1	0.004	456,094	0.324	0.31%
M5	0.1	0.003	489,624	0.324	0.00%

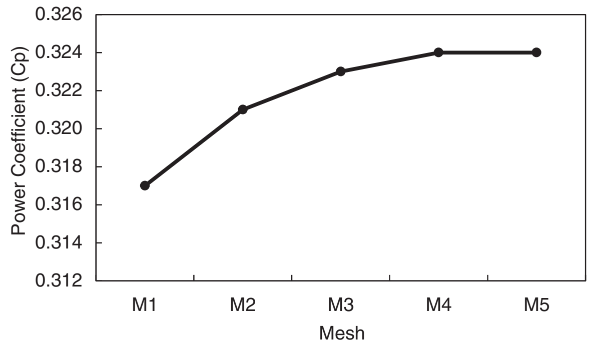

Figure 3: Mesh independence study for C_p at TSR = 3

2.4 Boundary Condition and Numerical Setting

The inlet in this study is located on the left boundary of the computational domain and has a velocity of 8 m/s, a turbulence intensity of 5%, and a turbulence ratio of 14%. These values are consistent with boundary conditions commonly used in CFD studies and validated through wind tunnel experiments and real-world wind conditions for VAWTs [31–35]. The right boundary of the domain is defined as a pressure outlet. The symmetry criteria are the upper and lower bounds of the fixed domain. Furthermore, A no-slip boundary condition is imposed on the surfaces of both the airfoil and the cylindrical deflector, treating them as walls where the fluid velocity at the boundary is set to zero. This condition ensures that the fluid adheres to the surface, reflecting the real physical interaction between the fluid and solid boundaries in CFD simulations. By applying this boundary condition, the development of the boundary layer and the calculation of aerodynamic forces can be accurately modeled, which is crucial for assessing the performance of aerodynamic structures like airfoils.

Previous studies have shown that the SST k-ω turbulence model is widely used for wind turbine simulations due to its accurate prediction of flow separation and transitional flow behavior, which are critical for VAWTs. A comparative analysis of seven commonly used turbulence models for VAWTs confirmed that only the SST model variants provided reliable results for turbine performance and blade aerodynamics, with the transitional SST k-ω models (SSTI and TSST) recommended as the most accurate for transitional flow regimes [33]. In this study, the SST k-ω model was selected to ensure reliable and accurate results, particularly in capturing the complex aerodynamic characteristics of the turbine.

The pressure-velocity coupling in ANSYS Fluent is implemented using the semi-implicit method for pressure linked equations (SIMPLE) method and a second-order implicit transient formulation. To guarantee accuracy, second-order upwind spatial discretization is applied to pressure, momentum, and turbulence equations. For solution stability, 10^{-5} is the convergence criterion. A 0.1° azimuthal increment is selected for the turbine's unsteady simulations, corresponding to a 0.0000363 s time step at TSR = 3. The criteria for several simulation situations are shown in Table 4, which also shows how this time step and rotational speed vary based on the TSR.

Table 4: Rotational speed and time step for different TSR

TSR	Rotational speed, ω (rad/s)	Time step, Δt
1.5	24	0.0000726
2.0	32	0.0000545
2.5	40	0.0000436
3.0	48	0.0000363
3.5	56	0.0000311

2.5 Mathematical Equations

Several mathematical equations were employed to evaluate the performance of the vertical-axis wind turbine (VAWT) in this study, focusing on the tip speed ratio (TSR), torque coefficient, C_m, and power coefficient, C_p. The TSR (λ) defines the ratio between the tangential speed of the turbine blade and the free-stream wind velocity, as shown in Eq. (1):

$$\lambda = \frac{\omega R}{U\infty} \tag{1}$$

where ω is the angular velocity of the rotor (rad/s), R is the turbine radius (m), and U_∞ is the free-stream wind velocity (m/s). The torque coefficient (C_m) quantifies the torque produced by the turbine relative to the dynamic pressure and rotor geometry, expressed in Eq. (2):

$$C_m = \frac{T}{\rho A R U_\infty^2} \tag{2}$$

where T is the torque (N·m), ρ is the air density (kg/m^3), A is the rotor swept area, and U_∞ is the free-stream wind velocity (m/s). Traditionally, the power coefficient, C_p is calculated using Eq. (3):

$$C_P = \frac{T}{\rho A R U_\infty^3} \tag{3}$$

However, in this study, C_p was determined using an alternative equation (Eq. (4)), which relates the power coefficient to the average torque coefficient and the tip speed ratio:

$$C_P = \lambda .Cm \tag{4}$$

This approach offers a more practical way to analyze the turbine's aerodynamic performance and assess its efficiency under different operating conditions.

3 Results and Discussion

3.1 Model Validation

The validation of the two-dimensional (2D) simulation confirmed that the conceptual model design adhered to the specified design parameters and that the predicted solutions were both accurate and applicable to practical scenarios. The second phase of the numerical study focused on validating the SST k-ω turbulence model. Solution parameters and boundary conditions for all validations were defined based on the experimental setup and CFD simulation data provided by Li et al. (2018), with a constant wind speed of 8 m/s [31].

As shown in Fig. 4, the 2D simulation results demonstrated a high degree of consistency with the experimental data for the target function C_p, with an estimated deviation of approximately 5% for TSR values up to 3. However, for TSR values greater than 4, the deviation increased to approximately 20%. This increasing deviation can be attributed to the growing influence of unsteady aerodynamic effects and the limitations of 2D simulations at higher tip speed ratios, where three-dimensional flow structures become more dominant and affect accuracy. These results are consistent with the findings of Jiang et al. (2020) and Bashir Ali Bashir et al. (2022), who reported similar deviations at higher TSRs due to complex flow structures and wake interactions [12,18]. In contrast, deviations of 15% and 30% were observed when compared with other references [36–38], indicating that the present computational results were more accurate than those reported in the evaluated literature.

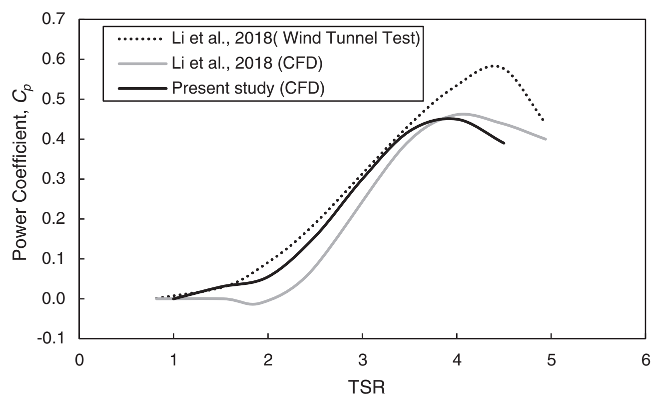

Figure 4: Change of C_p with TSR for present CFD model, compared to published CFD and experimental results [31]

3.2 Impact of the Cylindrical Deflector to the VAWT Performance

To investigate the effects of incorporating a cylindrical deflector within a turbine, simulations were conducted on the bare turbine configuration. The results indicated a negative torque initiating at approximately 165 degrees for the first blade at different TSRs, as depicted in Fig. 5. This figure illustrates the torque coefficient as a function of the azimuth angle across various tip speed ratios, TSRs. Further analysis of the total torque and the performance of the three blades at TSR = 3, presented in Fig. 6, corroborated the persistent presence of negative torque across all blades.

To mitigate these limitations, an inner cylindrical deflector was evaluated using multiple diameters: 0.2, 0.3, 0.5, and 0.7 m. The findings demonstrated that the deflector with a diameter of 0.3 m markedly enhanced the torque coefficient and overall turbine performance. This enhancement is illustrated in Fig. 7, which compares the torque coefficient at TSR = 3 with and without the cylindrical deflector across varying dimensions. Additionally, the power coefficient, C_p exhibited an increase of 15% following the integration of the cylindrical deflector, underscoring its efficacy in augmenting turbine efficiency.

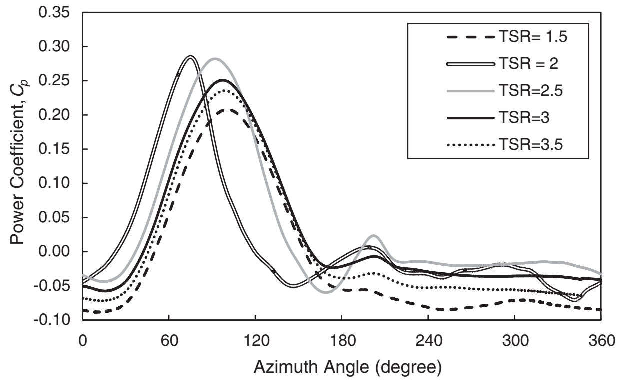

Figure 5: Torque coefficient for blade 1 against azimuth angle for various TSRs for an open turbine

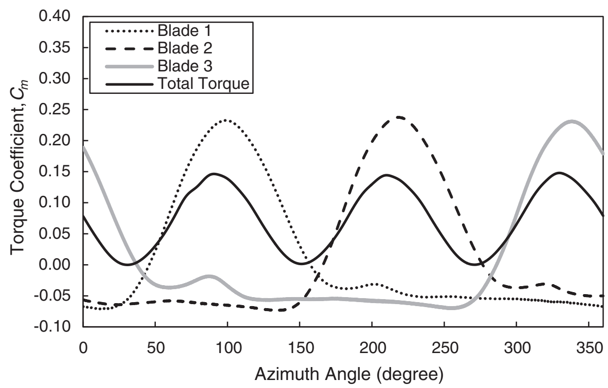

Figure 6: The three blades' torque coefficient against azimuth angle and the turbine's overall coefficient torque at TSR = 3

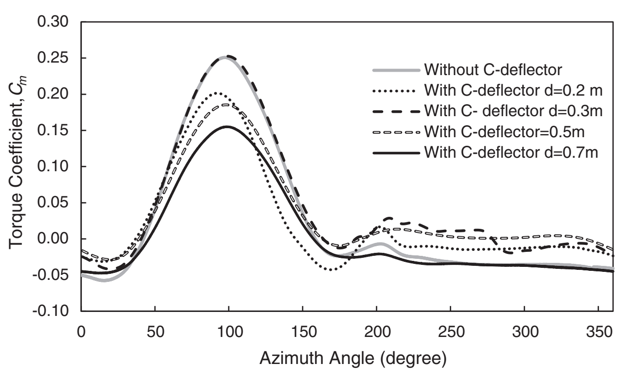

Figure 7: Torque coefficient for blade 1 against azimuth angle at TSR = 3 for both bare turbines and turbines with cylindrical deflectors of varying diameters

Furthermore, the velocity contours for both the bare turbines and turbines equipped with different cylindrical deflectors at TSR = 3 (Fig. 8) provide crucial insights into the aerodynamic improvements achieved. For the bare turbine, large stagnation zones are visible on the downwind side, particularly near the wake region, where flow separation occurs due to adverse pressure gradients.

This separation creates significant low-velocity regions and chaotic flow structures, which degrade aerodynamic performance and contribute to the formation of vortices that reduce torque production. The introduction of the cylindrical deflector alters the flow pattern around the turbine, redirecting and accelerating the airflow in a way that minimizes these stagnation regions and reduces turbulence intensity. Among the tested diameters, the 0.3 m deflector shows the most favorable results. It effectively streamlines the airflow, ensuring a more uniform velocity distribution around the blades and suppressing flow detachment on the downwind side. This reduction in wake turbulence not only improves the flow quality but also stabilizes the blade loading across the entire rotation cycle, leading to higher torque and improved power output. The organized flow downstream of the 0.3 m deflector results in a more coherent wake structure, which enhances the aerodynamic performance of the turbine.

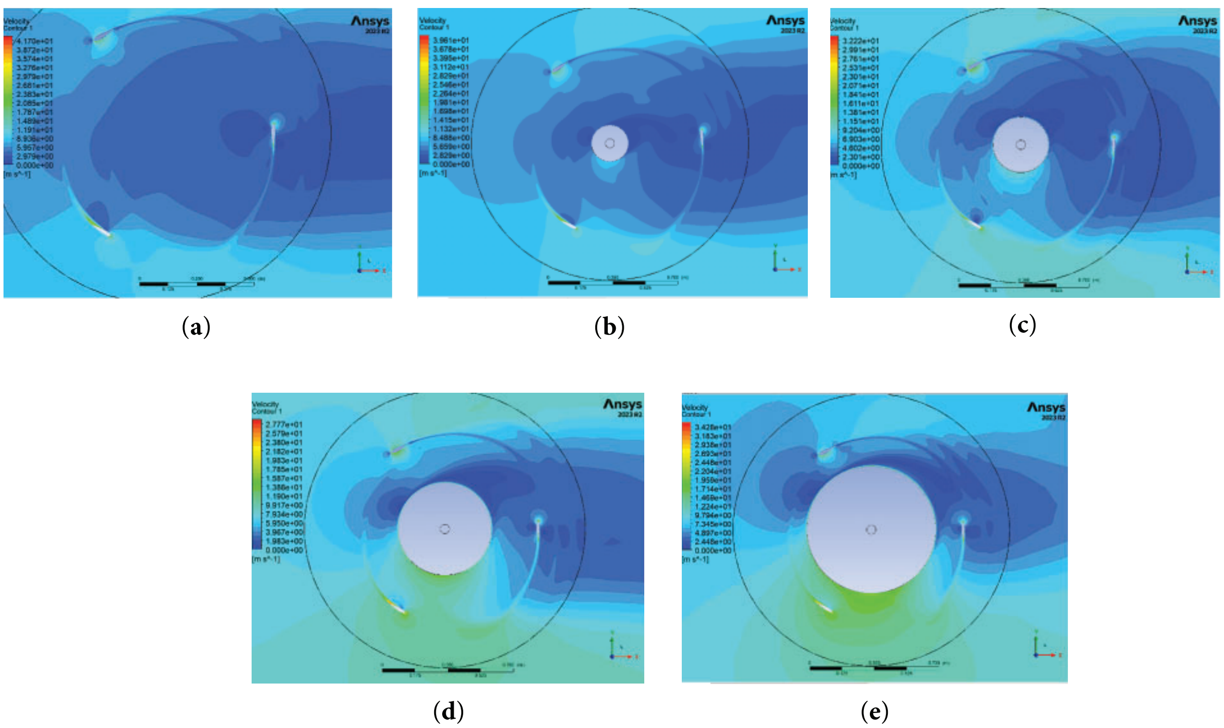

Figure 8: Velocity contours at 270° Azimuth angle for (a) bare turbine; (b) with deflector diameter = 0.2 m; (c) with deflector diameter = 0.3 m; (d) with deflector diameter = 0.5 m; (e) with deflector diameter = 0.7 m

On the other hand, the smaller 0.2 m deflector fails to provide sufficient blockage to control and redirect the flow effectively. Consequently, the velocity contours for this configuration show minimal improvement compared to the bare turbine. Significant regions of low velocity persist on the downwind side, resulting in limited performance gains. In contrast, the 0.7 m deflector introduces excessive flow blockage, causing a dramatic buildup of pressure on the upstream side of the deflector. This high-pressure zone disrupts the natural flow path and induces strong secondary flow structures, which lead to chaotic recirculation and velocity deficits in the downstream region. The resulting flow pattern is highly unsteady, leading to increased aerodynamic losses and reduced torque generation compared to the 0.3 m deflector. The 0.5 m deflector demonstrates intermediate performance, with velocity contours that closely resemble those of the bare turbine. While some reduction in stagnation regions is observed, the flow acceleration is not sufficient to significantly improve the torque coefficient or power output. This indicates that the deflector size is critical in achieving the desired flow control effects and that the 0.5 m deflector does not strike the optimal balance between flow acceleration and blockage reduction.

Overall, the results from Fig. 8 confirm that the 0.3 m cylindrical deflector provides the optimal combination of flow acceleration and uniform velocity distribution. This improved flow pattern reduces aerodynamic losses by maintaining a positive angle of attack across a larger portion of the blade's rotation, particularly in the downwind region where flow separation is most problematic. The more stable and coherent wake structure minimizes unsteady aerodynamic loading on the blades, contributing to the observed 15% increase in C_p (Fig. 9). These findings underscore the importance of selecting an appropriate deflector size to enhance turbine performance through targeted flow control strategies.

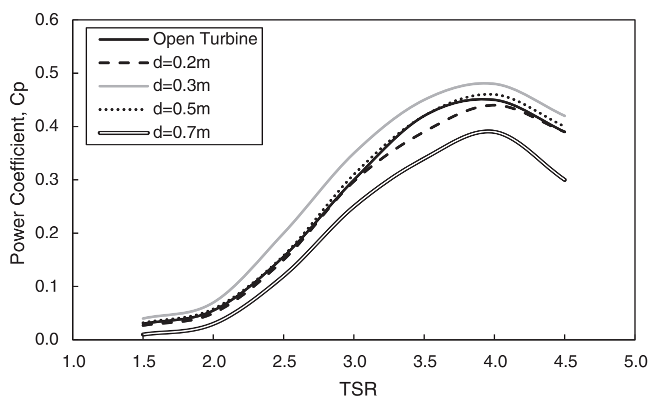

Figure 9: Power coefficient *vs*. TSR for both bare turbines and turbines with varying diameter cylindrical deflectors

4 Conclusions

This study investigates the impact of a cylindrical deflector on the performance of three-bladed VAWTs with modified airfoils. CFD simulations indicate that integrating the deflector significantly enhances turbine efficiency. Initial simulations of the bare turbine configuration show negative torque beginning at approximately 165 degrees of the azimuth angle. With the deflector in place, the power coefficient, C_p increases by about 15%, primarily due to improved airflow optimization around the blades, leading to reduced losses and enhanced torque generation.

The torque coefficient data, presented through multiple charts, highlights the performance differences between the bare turbine and the turbine equipped with a deflector. The turbine with the deflector exhibited enhanced torque production across all blades, indicating more consistent aerodynamic performance. Furthermore, the comparison of torque coefficients at various deflector sizes suggests that choosing the appropriately sized deflector is crucial for optimizing the turbine's performance.

In conclusion, this research underscores the potential of cylindrical deflectors as an effective design modification for enhancing the efficiency of vertical-axis wind turbines. The insights gained contribute significantly to the enhancement of wind turbine design, paving the way for the development of more efficient and cost-effective wind energy systems. Future studies should concentrate on further refining the geometry of the deflectors, conducting additional experimental validations, and investigating the influence of deflector placement on the overall efficiency of the turbine.

Acknowledgement: None.

Funding Statement: This research was funded by Ministry of Higher Education Malaysia under the Fundamental Research Grant Scheme (FRGS/1/2024/TK10/UKM/02/7).

Author Contributions: The authors confirm contribution to the paper as follows: Conceptualization, Najm Addin Al-Khawlani and Ahmad Fazlizan; methodology, Najm Addin Al-Khawlani and Zambri Harun; software, Ahmad Fazlizan; validation, Asmail A. M. Abdalkarem and Adnan Ibrahim; formal analysis, Najm Addin Al-Khawlani; investigation, Najm Addin Al-Khawlani; resources, Ahmad Fazlizan; data curation, Najm Addin Al-Khawlani and Asmail A. M. Abdalkarem; writing—original draft preparation, Najm Addin Al-Khawlani; writing—review and editing, Ahmad Fazlizan; visualization, Najm Addin Al-Khawlani; supervision, Ahmad Fazlizan and Adnan Ibrahim; project administration, Ahmad Fazlizan; funding acquisition, Ahmad Fazlizan. All authors reviewed the results and approved the final version of the manuscript.

Availability of Data and Materials: All data generated or analyzed during this study are included in this published article.

Ethics Approval: Not applicable.

Conflicts of Interest: The authors declare no conflicts of interest to report regarding the present study.

References

1. Nwokediegwu ZQS, Ibekwe KI, Ilojianya VI, Etukudoh EA, Ayorinde OB. Renewable energy technologies in engineering: a review of current developments and future prospects. Eng Sci Technol J. 2024;5(2):367–84. doi:10.51594/estj.v5i2.800.
2. Bai CJ, Wang WC. Review of computational and experimental approaches to analysis of aerodynamic performance in horizontal-axis wind turbines (HAWTs). Renew Sustain Energy Rev. 2016;63:506–19. doi:10.1016/j.rser.2016.05.078.
3. Boyd M, Jackson M, Jacobsen AC, Lackie J, Rosica P, Savilonis B. Articulating Wind Turbine. : Worcester Polytechnic Institute; 2015 [cited 2025 Feb 18]. Avilable from: https://digital.wpi.edu/concern/student_works/jq085m540?locale=de.
4. Zoucha J, Crespo C, Wolf H, Aboy M. Review of recent patents on vertical-axis wind turbines (VAWTs). Recent Pat Eng. 2022;17(4):e290822208177. doi:10.2174/1872212117666220829143132.
5. Chong WT, Muzammil WK, Ong HC, Sopian K, Gwani M, Fazlizan A, et al. Performance analysis of the deflector integrated cross axis wind turbine. Renew Energy. 2019;138:675–90. doi:10.1016/j.renene.2019.02.005.
6. Almalki H, Safaei B, Karimzadeh Kolamroudi M, Sahmani S, Arman S, Shekoofa O. Systematic literature review on the design, efficiency and fabrication of wind turbine blades. Int J Am Energy. 2024;45(1):2374057. doi:10.1080/01430750.2024.2374057.
7. Ahmad M, Shahzad A, Qadri MNM. An overview of aerodynamic performance analysis of vertical axis wind turbines. Energy Environ. 2023;34(7):2815–57. doi:10.1177/0958305X221121281.
8. Elsakka MM, Ingham DB, Ma L, Pourkashanian M. CFD analysis of the angle of attack for a vertical axis wind turbine blade. Energy Convers Manage. 2019;182:154–65. doi:10.1016/j.enconman.2018.12.054.

9. Das Karmakar S, Chattopadhyay H. A review of augmentation methods to enhance the performance of vertical axis wind turbine. Sustain Energy Technol Assess. 2022;53:102469. doi:10.1016/j.seta.2022.102469.
10. Hand B, Kelly G, Cashman A. Aerodynamic design and performance parameters of a lift-type vertical axis wind turbine: a comprehensive review. Renew Sustain Energy Rev. 2021;139:110699. doi:10.1016/j.rser.2020.110699.
11. Wong KH, Chong WT, Poh SC, Shiah YC, Sukiman NL, Wang CT. 3D CFD simulation and parametric study of a flat plate deflector for vertical axis wind turbine. Renew Energy. 2018;129:32–55. doi:10.1016/j.renene.2018.05.085.
12. Jiang Y, Zhao P, Stoesser T, Wang K, Zou L. Experimental and numerical investigation of twin vertical axis wind turbines with a deflector. Energy Convers Manage. 2020;209:112588. doi:10.1016/j.enconman.2020.112588.
13. Vijay MBP, Bharat MJS, Shamrao MTY, Lalit MTT, Suresh PPS. Experimental analysis of vertical axis wind turbine. Int J Res Appl Sci Eng Technol. 2023;11(5):7303–6. doi:10.22214/ijraset.2023.53458.
14. Iliev R, Tsalov T. Investigation of a cross-flow wind turbine with a hybrid frontal guiding device. IOP Conf Ser: Earth Environ Sci. 2024;1380(1):012001. doi:10.1088/1755-1315/1380/1/012001.
15. Wang XH, Wong KH, Chong WT, Ng JH, Qiu CJ, Khor CS. Performance evaluation of a downwind diffuser on vertical axis wind turbine. Int J Energy Res. 2022;46(1):351–69. doi:10.1002/er.6890.
16. Wang WY, Ferng YM. Numerical model for noise reduction of small vertical-axis wind turbines. Wind Energ Sci. 2024;9(3):651–64. doi:10.5194/wes-9-651-2024.
17. Abbasi S, Daraee MA. Improving vertical-axis wind turbine performance through innovative combination of deflector and plasma actuator. Phys Fluids. 2024;36(4):045134. doi:10.1063/5.0204070.
18. Bashir Ali Bashir M, Ali I, Hussain Rajpar A. Performance analysis of micro-vertical axis wind turbine integrated with upstream omnidirectional wind deflector. Arab J Sci Eng. 2022;47(12):16239–49. doi:10.1007/s13369-022-06896-1.
19. Yan Y, Zhang J, She J, Liu W, Deng J, Zhu J. Effect of additional cylinders on power-extraction performance of a Savonius vertical-axis wind turbine. J Zhejiang Univ Sci A. 2023;24(6):531–42. doi:10.1631/jzus.A2200292.
20. Chen WH, Lam TT, Chang MH, Jin L, Chueh CC, Augusto GL. Optimizing H-darrieus wind turbine performance with double-deflector design. Energies. 2024;17(2):503. doi:10.3390/en17020503.
21. Tanino T, Yoshihara R, Miyaguni T. A study on a casing consisting of three flow deflectors for performance improvement of cross-flow wind turbine. Energies. 2022;15(16):6093. doi:10.3390/en15166093.
22. Kołodziejczyk K, Ptak R. Numerical investigations of the vertical axis wind turbine with guide vane. Energies. 2022;15(22):8704. doi:10.3390/en15228704.
23. Al-Gburi KAH, Alnaimi FBI, Al-Quraishi BAJ, Tan ES, Kareem AK. Enhancing savonius vertical axis wind turbine performance: a comprehensive approach with numerical analysis and experimental investigations. Energies. 2023;16(10):4204. doi:10.3390/en16104204.
24. Habibullah, Khan MA, Atif M, Ahmad S, Awwad FA, Ismail EAA. Numerical analysis of airfoils used in an omni-directional-guide vane structure of vertical axis wind turbine for high-rise buildings. Mod Phys Lett B. 2024;38(16):2341019. doi:10.1142/S0217984923410191.
25. Wong KH, Chong WT, Sukiman NL, Shiah YC, Poh SC, Sopian K, et al. Experimental and simulation investigation into the effects of a flat plate deflector on vertical axis wind turbine. Energy Convers Manage. 2018;160:109–25. doi:10.1016/j.enconman.2018.01.029.
26. Syawitri TP, Yao Y, Yao J, Chandra B. A review on the use of passive flow control devices as performance enhancement of lift-type vertical axis wind turbines. Wires Energy Environ. 2022;11(4):e435. doi:10.1002/wene.435.

27. Miliket TA, Ageze MB, Tigabu MT. Aerodynamic performance enhancement and computational methods for H-Darrieus vertical axis wind turbines: review. Int J Green Energy. 2022;19(13):1428–65. doi:10.1080/15435075.2021.2005605.
28. Zhang L, Zhu K, Zhong J, Zhang L, Jiang T, Li S, et al. Numerical investigations of the effects of the rotating shaft and optimization of urban vertical axis wind turbines. Energies. 2018;11(7):1870. doi:10.3390/en11071870.
29. Rezaeiha A, Kalkman I, Blocken B. Effect of pitch angle on power performance and aerodynamics of a vertical axis wind turbine. Appl Energy. 2017;197:132–50. doi:10.1016/j.apenergy.2017.03.128.
30. Deslot C, Kulisa P, Bario F. Numerical investigation on potential effects induced by rotor-*Stator* interaction in an axial turbine. Int Rev Modell Simul. 2008;1:355–64.
31. Li C, Xiao Y, Xu YL, Peng YX, Hu G, Zhu S. Optimization of blade pitch in H-rotor vertical axis wind turbines through computational fluid dynamics simulations. Appl Energy. 2018;212:1107–25. doi:10.1016/j.apenergy.2017.12.035.
32. Jooss Y, Hearst RJ, Bracchi T. Influence of incoming turbulence and shear on the flow field and performance of a lab-scale roof-mounted vertical axis wind turbine. J Renew Sustain Energy. 2023;15(6):063302. doi:10.1063/5.0170059.
33. Rezaeiha A, Montazeri H, Blocken B. On the accuracy of turbulence models for CFD simulations of vertical axis wind turbines. Energy. 2019;180:838–57. doi:10.1016/j.energy.2019.05.053.
34. Zamre P, Lutz T. Computational-fluid-dynamics analysis of a Darrieus vertical-axis wind turbine installation on the rooftop of buildings under turbulent-inflow conditions. Wind Energ Sci. 2022;7(4):1661–77. doi:10.5194/wes-7-1661-2022.
35. Gerrie C, Islam SZ, Gerrie S, Turner N, Asim T. 3D CFD modelling of performance of a vertical axis turbine. Energies. 2023;16(3):1144. doi:10.3390/en16031144.
36. Shahizare B, Nazri Bin Nik Ghazali N, Chong W, Tabatabaeikia S, Izadyar N. Investigation of the optimal omni-direction-guide-vane design for vertical axis wind turbines based on unsteady flow CFD simulation. Energies. 2016;9(3):146. doi:10.3390/en9030146.
37. Yang Y, Cao Y, Qian Z, Wang J, Zhu Y, Chen X, et al. A study on the effect of turbulence intensity on dual vertical-axis wind turbine aerodynamic performance. Energies. 2024;17(16):4124. doi:10.3390/en17164124.
38. Ansaf R, Abdelhameed HS, Hashem I, Harun Z. Efficiency-based design optimization of the H-type Darrieus wind turbine with fixed guiding-walls. Energy Rep. 2023;9:3576–92. doi:10.1016/j.egyr.2023.01.117.